2018

WOM: Whole ORC Model

Saverio Randi
University of Ferrara, via Saragat 1, 44122 Ferrara – ITALY, saverio.randi@unife.it

Nicola Casari
University of Ferrara, Italy, nicola.casari@unife.it

Michele Pinelli
University of Ferrara, michele.pinelli@unife.it

Alessio Suman
University of Ferrara, alessio.suman@unife.it

Davide Ziviani
School of Mechanical Engineering, Ray W. Herrick Laboratories, Purdue University, dziviani@purdue.edu

WOM: Whole ORC Model

Saverio RANDI[1]*, Nicola CASARI[1], Michele PINELLI[1], Alessio SUMAN[1], Davide ZIVIANI[2]

[1]University of Ferrara,
Via Saragat 1, 44122 Ferrara, Italy
saverio.randi@unife.it, nicola.casari@unife.it, michele.pinelli@unife.it, alessio.suman@unife.it

[2] Ray W. Herrick Laboratories, Purdue University,
177 S Russell Street, West Lafayette, IN, 47907-2099, USA
dziviani@purdue.edu

* Corresponding Author

ABSTRACT

Over the last decade, environmental and economic concerns have pushed the researchers to find new solutions in the track of a more responsible use of energy. Particularly, small scale organic Rankine cycles (ORCs) have been regarded as candidates for a better employment of waste energy. In order to increase the performance of these cycles and to extend their operating range, attention has been drawn on the behavior of the different components both experimentally as well as numerically. The numerical approach has been increasingly used in the study of the machines that compose the cycle, to overcome some limitations experimental analyses have (e.g. compatibility of refrigerant with sealing systems) and allowing for the preliminary test of new machines to be added to the cycle.

In this work, a virtual test bench called Whole ORC Model (WOM) is developed demonstrating the possibility to use the numerical analysis, not only for the study/optimization of a single, stand-alone component, but also for improving the comprehension on their reciprocal interaction, and thus, the performance of the single part and on the entire system. Such a virtual model can be of paramount importance in predicting the behavior of the cycle in off-design conditions or in gathering information about fluid stagnation locations. A preliminary assessment of an actual ORC system is reported with the goal of demonstrating the possible analyses and results. In the future, WOM can be extended in order to couple the ORC system with the external world. Specifically, the grid demand and the heat flux at the evaporator can vary: such changes can be translated in a variation in the boundary conditions. The response of the cycle to the external variation can be therefore monitored and studied.

1. INTRODUCTION

It is known that ORC systems represent a useful way to recover low-grade heat from different types of applications, characterized by different levels of complexity (Macchi and Astolfi, 2016). Control strategies of each of these systems are strongly affected by their dynamic behavior, which can be studied in different ways, including computational fluid dynamic (CFD). This tool is useful to improve the ORC performance during the design process or to assess the behavior of an existing cycle when boundary conditions are changed. Nowadays, CFD has been applied to the design and analysis of the single components of the cycle (compressor, expanders and heat exchangers, as showed by Bhutta *et al.* 2012, Chang *et al.* 2014, Morini *et al.* 2015, Song *et al.* 2015, Ziviani *et al.* (2016), Casari *et al.* 2017a-b, Suman *et al.* 2017). The difficulties in this case are related to the simulation of the positive displacement machines (that usually equip micro ORC systems as reported in Macchi and Astolfi, 2016) for which the CFD analysis must be able to accommodate the variation of the chamber volume and shape over the machine revolution.
However, the growing computational resources make the numerical simulations of these machines affordable (in terms of computational time) even during the design phase, or in other cases, able to solve very complex features like volume variation inside a complex positive displacement machines as twin (Papes *et al.*, 2015) and single

(Ziviani *et al.*, 2016) screw expanders, observe the onset and development of cavitation phenomena in pumps (Del Campo *et al*., 2012), verify how machine performances are affected by fluid leakages due to gaps between stationary and moving parts (Castilla *et al*., 2010) or visualize condensation and evaporation mechanisms inside heat exchangers.

The analysis of the single components is only a part of the approach to the problem: when evaluating whole system behavior, the interaction between these parts has to be considered. In this case, the use of CFD is uncommon: for example, Donghong *et al.* (2008) used Dymola® to simulate the transient behavior of a pilot ORC system, Dickes *et al.* (2017) predicted the performance of a test rig operating in off-design conditions by using three different lumped parameter modelling paradigms, in order to find the best compromise between robustness, accuracy and complexity. These numerical approaches are adopted in numerous studies, such as the ones implemented to analyze the behavior of the system as a function of the charge of the fluid (Liuchen *et al.*, 2017) or that by Desideri *et al.* (2014), in which a model was developed to take into account the steady state behavior of the whole system.

In light of these considerations, the virtualization of the whole ORC model can be carried out in order to build a virtual test bench: such a device can be useful for testing the off-design conditions rather than mapping the performance of each component and the reciprocal interaction during transient behavior (Casari *et al.*, 2017c). A very interesting piece of information that can be extracted from this approach is the location where the liquid charge stops and/or the modification of the ORC performance related to the charge migration of refrigerant. In addition, control strategies and evaluation of the most appropriate measurement points can be determined by employing the proposed approach.

In this paper, a 3D transient CFD model of a non-recuperative ORC has been carried out. The sizing of the various components of the cycle has been done by considering the dimensions of the parts installed in a test cycle installed at University of Bologna facilities. The experimental characterization of this system has already been shown by Ancona *et al*. (2016) and Bianchi *et al*. (2017a-b), so data for pressure and temperatures at the inlet and outlet of the various components are available, as well as mass flow rate of the working fluid, which is R134a. In this way, it has been possible to choose one working point from which one can obtain the boundary conditions of the computational model. The distribution of the fluid inside the circuit is then exploited by running a transient simulation, starting from a configuration in which the heat exchangers are filled with both liquid and gas. The simulations have been carried out with Simcenter STAR-CCM+®. Information about heat exchange and liquid-to-gas fraction are also depicted. Given this, the present work develops according to the following points:

- geometrical and thermodynamic analysis of an actual ORC system comprising refrigerant, heat sources, device volumes, pump and expander;
- virtualization and simplification of an actual ORC system, with particular attention to phase change resolution;
- selection and implementation of the proper numerical models for reproducing cycle operation, such as boiling, expansion and condensation phases;
- transient simulation and data post process.

2. MICRO ORC LAYOUT

The reference ORC system is depicted in Figure 1 where the installation at the University of Bologna facility (Figure 1a) and the P&ID scheme (Figure 1b) are reported. This ORC systems is a recuperative-type cycle and it is equipped with a radial three piston expander with a nominal power equal to 3 kWe. In addition, an inverter operated volumetric gear pump, which controls the mass flow of organic fluid in the circuit is installed. A brazed plate heat exchanger acts as the evaporator, while a shell and tube heat exchanger guarantees the organic fluid condensation. Hot and cold water are used as heat source and sink, respectively.

The cycle is monitored with several T-type thermocouples and ceramic pressure transducers to collect data for temperature and pressure respectively, for monitoring the operating point of the ORC system and, at the same time, to characterize each device. The mass flow rate is precisely monitored by means of a Coriolis flow meter. From the experimental campaign, the operating point used in the present work has been taken.

3. SIMULATION SET-UP

3.1 Cycle model and its virtualization

Given the objective of the present work, the actual ORC system reported in Figure 1, was virtualized considering the

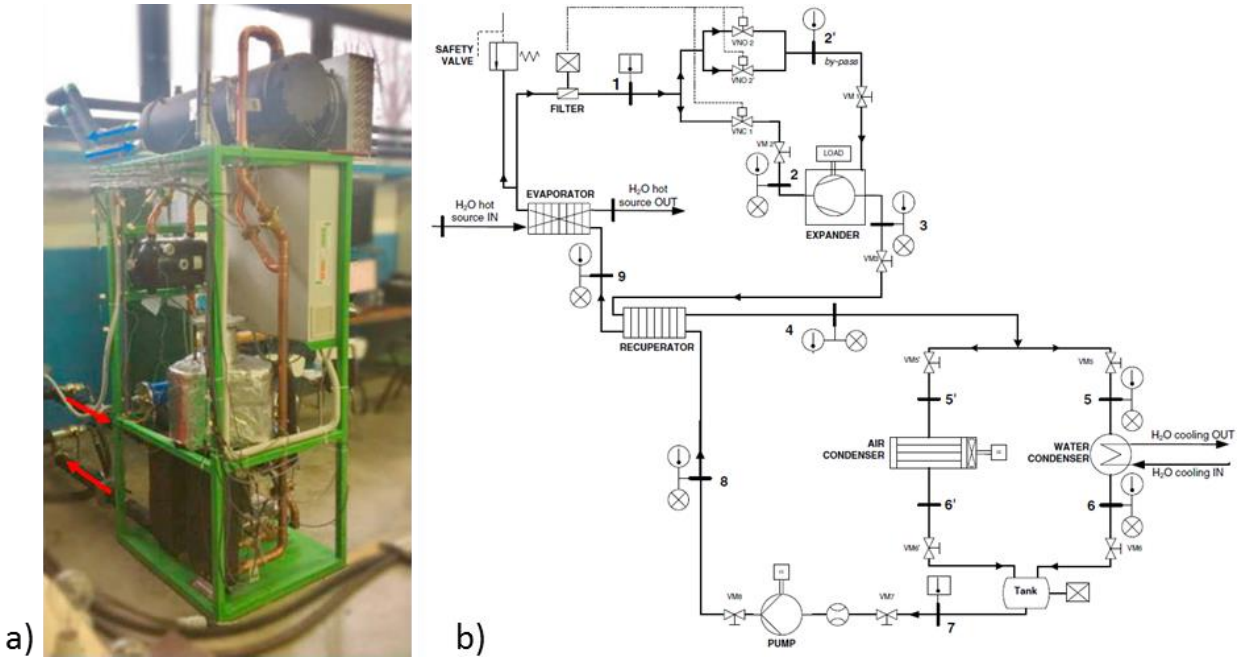

Figure 1: An actual recuperative ORC system: a) installation at the facility (Bianchi *et al.*, 2017b), b) P&ID

needs related to fast-and-reliable multiphase calculations. For this reason, several simplifications have been adopted for expander, pump and heat exchangers. With the reference of Figure 2, the CFD model comprises an evaporator, an expander (pressure-reducing valve), a condenser and a tank. The virtual model of the ORC system reflects the actual dimension. Globally, it is 2.7 m-high and 1.7 m-wide. Figure 2 depicts the ORC virtual layout numbered according to P&ID of Figure 1b.

Describing the Figure 2 from the left-hand side, the liquid fluid enters from the bottom into the evaporator, it boils, and it reaches the expander, which is preceded and followed by some fins to prevent flow pulsations in the duct, which is likely to occur during the simulation, and may be detrimental for its stability. The pressure-reducing valve in fact, is fixed and designed for a certain mass flow rate and gas density. This implies that, in the case of flow pulsation, the convergence history may get worse and eventually unstable. After the expander, the gas reaches the condenser and finally it is collected in the tank.

Focusing on the single components, the evaporator and condenser have been designed in order to have the same volume of the actual components. The geometry of the heat exchangers is made of a series of coaxial rectangular-sectioned tubes, describing sixteen surfaces which permit heat exchange. A cut section of the evaporator is showed in Figure 2. Condenser is similar to this part, except that its volume is nearly nine times greater (it reflects the fact that it is a shell and tube exchanger, while the former is a plate type). The arrangement of these components in the numerical model (vertical position) has been chosen to accommodate the change of state of the working fluid, considering the direction in which gravity force acts.

For what concerns the expander geometry, an assumption has been introduced: to test the proposed model, a simple pressure reducing valve has been considered. The simulation of a positive displacement machine is considered as a next step in this track. The capability of the software suite in positive displacement machine modeling has been already proven (Suman *et al.*, 2017).

Similar approach is adopted for the pump. This component has not been modeled but it is considered as a black-box. At the inlet and outlet of the virtual circuit, the conditions at the suction and discharge of the pump are imposed. The last component outlined in the circuit is the tank: it is necessary to create a buffer between the condenser and the pump in order to ensure an adequate head and to avoid gas phase at the suction of the volumetric machine. In addition to this, great care has been taken in designing a whole cycle model which could guarantee fast solution initialization and convergence, since the objective of this work is to assess the feasibility of such a CFD model.

Finally, bends, valves, pressure and temperature taps as well as the tube fittings have been neglected and not numerically modeled. Moreover, inlet and outlet sections of the heat exchangers have been designed in order not to have, or minimize, recirculation of the fluid coming to or leaving the component (divergent and convergent layout, respectively). In the Table 1, the main characteristics of the cycle divide according to each component have been reported.

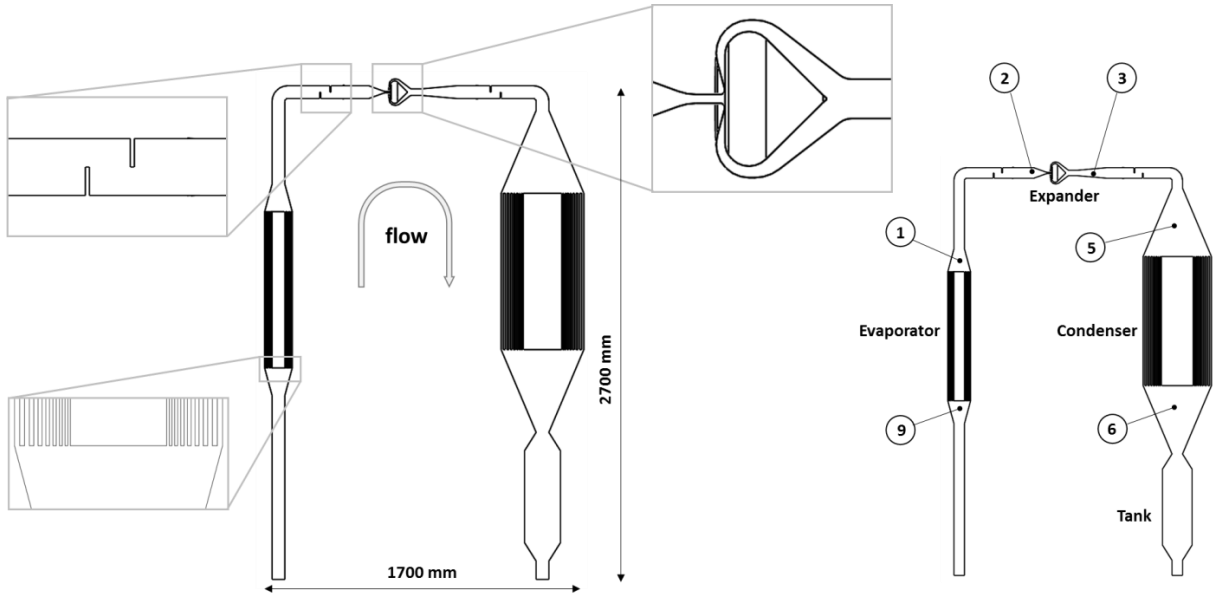

Figure 2: Numerical domain

Table 1: Components properties

Evaporator	Number of heat exchange surfaces	16
	Heat exchange area [m^2]	5.710
	Volume [l]	8.10
Expander	Expansion ratio	2
	Valve lift [mm]	0.3
Condenser	Number of heat exchange surfaces	16
	Heat exchange area [m^2]	17.13
	Volume [l]	72.9
Piping	Hydraulic diameter [m]	0.0694

3.2 Numerical models

The main challenges involved in the WOM approach analyzed in the present work, are related to the mass and heat transfer. In order to reduce the computational effort, the ideal gas model has been adopted. The phase change has been taken into account by means of Volume of Fluid (VOF) and fluid film evaporation/condensation models. In this section these approaches are explained.

The VOF method is suited to model multiphase flows under the assumption that all phases share pressure, temperature and velocity fields, as described by Hirt and Nichols (1981). It is based on an Eulerian representation of the problem and, to locate the interface between the phases, it introduces a function whose average value identifies the volume of fraction of fluid in a certain computational cell. Thus, when a cell contains a free surface, the value of this function stays between zero (no fluid) and one (fluid only). In addition to this information, another useful one is given by the direction in which function value varies most rapidly: in this way, also the direction in which the free surface moves is known. By knowing these two aspects of the flow, the interface between the phases can be approximated, for each grid element.

In the current work, the use of VOF approach has been suggested by the presence of both stratified and mixed flows inside the two heat exchangers. For transitional flows, since the size of computational cell would be excessively small, it has been necessary to couple the VOF method with the fluid film (FF) model by means of the resolved fluid film model. This approach governs the transition between FF and VOF phase thanks to a user-defined transition volume fraction value: when liquid volume fraction in the FF neighboring cell is greater than the value imposed by the user, fluid film transitions into the VOF phase and vice versa. This FF approach is needed to model the evaporating fluid in the evaporator and the condensing one in the condenser: the so-called *shell regions* must be

created on those model surfaces on which fluid is expected. In our case, these regions were positioned on the heat exchanging surfaces, where fluid changes its state and can also be transformed in a pool of liquid (such as evaporator inlet or condenser outlet). FF model solves transport equations for mass, momentum, energy and volume fraction, in order to calculate FF thickness, distribution, pressure, temperature and the film volume fraction in the neighboring cells, which is subtracted from the volume of the gas phase in the cells near the film. To account for the immiscibility of liquid and gas, surface tension on the interface has to be calculated; in addition, also the influence of the walls must be considered, by means of the definition of the contact angle between the liquid and the wall.
In Table 2 the values adopted for the current simulation are reported. The transient simulation was performed by employing a compressible solver able to cope with multiphase flow and interface tracking. A fixed time-step value is adopted equal to 1e-6 s while, for the turbulence modeling, a one-equation model of Spalart and Allmaras (1992) is chosen.

3.3 Mesh

A 21.5 million, polyhedral mesh has been generated to discretize the numerical domain. Mesh was refined in locations such as gaps between heat exchanging surfaces in evaporator and condenser, as well as in the expander throat. To improve the stability of the solution and model with greater accuracy heat transfer process to the fluid, in the heat exchangers passages five prism layers of cells were defined, with a total height of 1 mm (first cell centroid at 36 µm from the wall). Elements dimensions in the rest of the domain were greater (up to 5 mm), not to increase the total number of elements, while maintaining y^+ values in the range required for an all-y^+ approach (values less than one requires the solution of the viscous sub-layer, while values outside the transition zone are modeled thanks to wall functions). Two particular of the expander and the evaporator meshes are reported in Figure 3.

4. RESULTS

A transient analysis of 90 physical seconds of operation has been carried out. After this time the simulation has converged, reaching a steady state solution, due to the steady state condition of the heat source/sink and to the stationary operation of the expander. After this time the pressure and temperature distributions inside the ORC cycle are evaluated and reported in Figure 4.

Table 2: Model boundary conditions and fluid properties evaluated and the evaporator inlet section (for liquid) or condenser wall (for vapor)

Property	**Value**	**Property**	**Value**
Evaporator Wall Temperature [K]	351.0	Liquid Specific Heat [J/kg K]	1458.5
Evaporator Heat Transfer Surface [m^2]	5.71	Liquid Density [kg/m^3]	1172.3
Condenser Wall Temperature [K]	283.2	Liquid Viscosity [Pa s]	1.744e-4
Condenser Heat Transfer Surface [m^2]	17.13	Liquid Thermal Conductivity [W/m K]	0.07749
Liquid Mass Flow Rate [kg/s]	0.1	Vapor Specific Heat [J/kg K]	1235.0
Liquid Inlet Temperature [K]	308.6	Vapor Density [kg/m^3]	82.85
Liquid Inlet Pressure [MPa]	1.8	Vapor Viscosity [Pa s]	1.437e-5
Liquid-gas Surface Tension [N/m]	4.6100e-3	Vapor Thermal Conductivity [W/m K]	0.01919

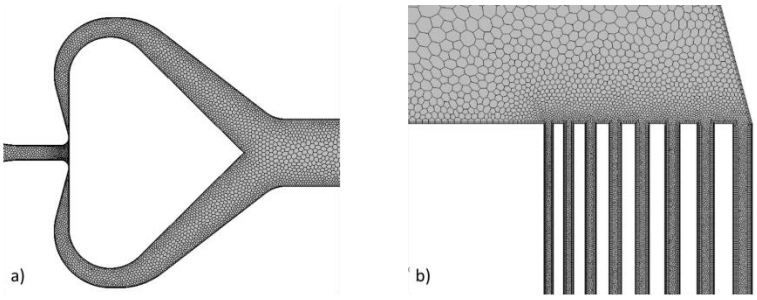

Figure 3: Details of the computational grid: a) expander and b) evaporator

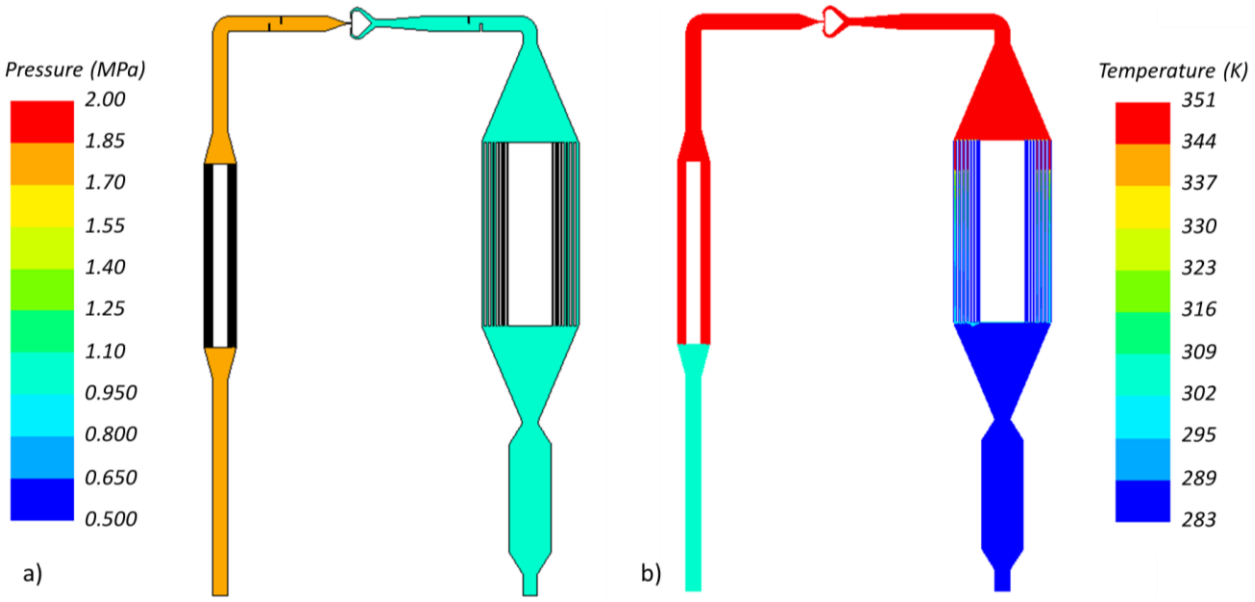

Figure 4: Overall results: a) pressure field, b) temperature field

In Figure 4a, the pressure distribution is reported. It can be clearly seen that each of the branches (evaporator and condenser ones) is at uniform pressure. The pressure jump is concentrated at the expander that works at a pressure ratio around 1.7. The distributed pressure losses are the responsible of the difference with the head: more quantitative results on the pressure losses across each component and along the piping are reported in Table 3. The distributed pressure losses along the piping are layout-dependent: the advantage of the proposed model is that it can catch such phenomenon.

Figure 4b reports the temperature field inside the ORC. Before the evaporator and after the condenser the temperature is uniform (and equal to the pump outlet and inlet respectively). This entails a temperature increase due to the pump of around 25 K. This temperature jump is remarkably high for the common applications and it is due to the fact that the fluid is extremely subcooled. This choice has been made in order to be sure to have pure liquid at the receiving tank, and it is not of concern for the purpose of this work. The local value upstream and downstream from every component is reported in Table 3.

The ORC plants are always equipped with a control system that is responsible for the proper working of the ORC itself. Table 3 reports data taken with a numerical probe, as it may be done by pressure/temperature probes. This kind of data is very useful when the control system has to be set-up: the WOM approach may be very helpful in the calibration of the control system as well.

In Table 3, enthalpy and entropy calculated from the CFD data through the REFPROP v7 library. These state functions are often employed to represent the cycle on the thermodynamic diagram. Figure 5 is representative of the transformations that happen in the cycle. The numbers are the same of Table 3 and of the P&ID reported in Figure 1b. The over-exaggerated subcooling of the liquid is particularly clear from Figure 5 (the point 6 is very close to the pump suction port). The blue and red lines represent the saturated vapor and saturated liquid lines

Table 3: Pressure, temperature and enthalpy results at the inlet/outlet sections

Sections	p [bar]	T [K]	h [kJ/kg]	s [kJ/kg K]
9- Evaporator IN	17.73	308.6	249.59	1.1664
1- Evaporator OUT	17.71	350.3	446.73	1.7582
2- Expander IN	17.69	349.5	445.78	1.7555
3- Expander OUT	10.15	349.1	457.97	1.8278
5- Condenser IN	10.12	349.0	457.91	1.8278
6- Condenser OUT	10.08	283.2	213.75	1.0474

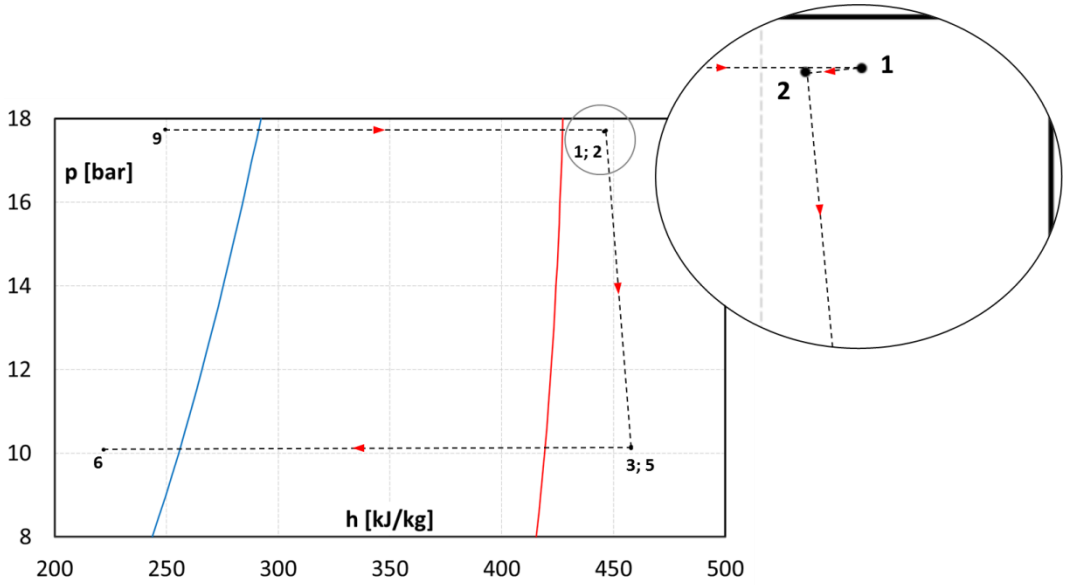

Figure 5: p-h diagram of the ORC and particular of the evaporator-expander duct transformation

respectively. This may be considered as the input that is given at the control system of the ORC: unexpected transformations like 1-2 is reported in the enlarged area at the right-hand side of Figure 5.

Here, the pressure losses due to the piping that connects the evaporator to the expander make the pressure to lower. In addition to the distributed pressure losses, the fins that are installed to prevent pressure waves to travel upstream making the simulation unstable involve an extra pressure drop. This pressure drop is responsible for the enthalpy reduction together with a reduction in the temperature as one can derive from Table 3. Such lower temperature is given by two main reasons. Firstly, mixing phenomena that uniform the temperature (the probe is located immediately downstream the heat exchanger and thus its value is affected by the hot streaks). Secondly, the cross section of the duct varies and an acceleration in the flow field converts the static temperature in dynamic contribution.

A parameter that may be of interest for predicting the behavior of the heat exchanger is the temperature evolution along the plate. This graph, reported in Figure 6, gives information about the quality of the saturated vapor inside the heat exchanger and is very helpful to monitor the state of the exchangers (e.g. the heat transfer coefficient distribution or peak) or when an off-design condition (e.g. a lower temperature heat source) is to be handled. For example, in this work a peak $\alpha \sim 6000$ W/m^{2}K for the evaporator has been found, and $\alpha \sim 2000$ W/m^{2}K for the condenser.

Figure 6a reports the temperature evolution along the nondimensional axial coordinate of the evaporator. The asymptotic value equal to the imposed wall temperature (T_{wall}) is reached after z=0.5. The perhaps unexpected shape of the diagram is related to the fact that the phase change (PC) happens in a very small region: the high exchanger surfaces make the boiling region very localized. The same reasoning applies for Figure 6b, where the condenser is

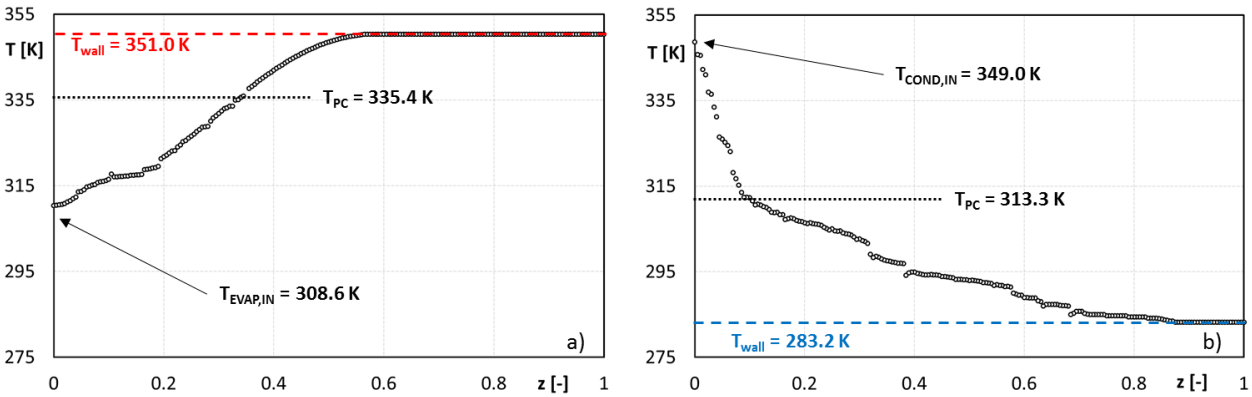

Figure 6: Temperature evolution inside the heat exchangers: a) evaporator b) condenser

considered. Again, the large amount of superheating and subcooling was introduced to ease the convergence of the numerical simulation.
The results reported in Figure 6 are confirmed if one considers the relative fraction of gas and liquid reported in Figure 7. Both the evaporator and the condenser are oversized as can be seen from the area where the phase change happens. The evaporator is almost totally occupied by gas fraction and the liquid floods only a very small portion.
The opposite can be stated for the condenser: the liquid is present in a large part of the device. This remark is of paramount importance when the operator is interested in the location where the liquid charge stops: by monitoring the liquid fraction one can estimate the amount of such phase in each of the component of the cycle, thus the weight of each component. For example, in the case under investigation, the condenser volume is around 73 l. Of these, during the steady state operation, 47.7 l (65 % of the total volume) are flooded by the liquid. The saturated vapor occupies 12.4 l (17 %) and the 12.9 l (18 %) left are occupied by gas.

6. CONCLUSIONS

In this paper, the first application of the WOM framework is presented. An actual ORC system has been taken into consideration to obtain the reference geometry and operating conditions (mass flow rate, pressure and temperature values and the working fluid R134a). To test the phase change models, which represent one of the biggest issues in the numerical modeling of the cycle operation, the system has been simplified (the pump has been removed and pressure reducing valve is used as expansion device).
The use of WOM approach allows the evaluation of several peculiarities of an ORC system. Pressure drops, local temperature variation (cold/hot spots), heat exchangers performance are only few of the results that can be extracted by employing the proposed model.
WOM can be useful to get on-board information for, the conductor of the power plant (e.g. for maintenance planning), the control system set-up (e.g. for off-design conditions) and the manufacturer (e.g. for performance predictions). At the same time, such virtual model can be applied for multiple purposes as (i) the recognition of particular phenomena that involve each device such as liquid level, (ii) the variation of the working fluid avoiding the issues related to the compatibility with the sealants and lubricant and (iii) testing the overall behavior during off-design operation or when cycle modification has to be tested (e.g. trilateral cycles).

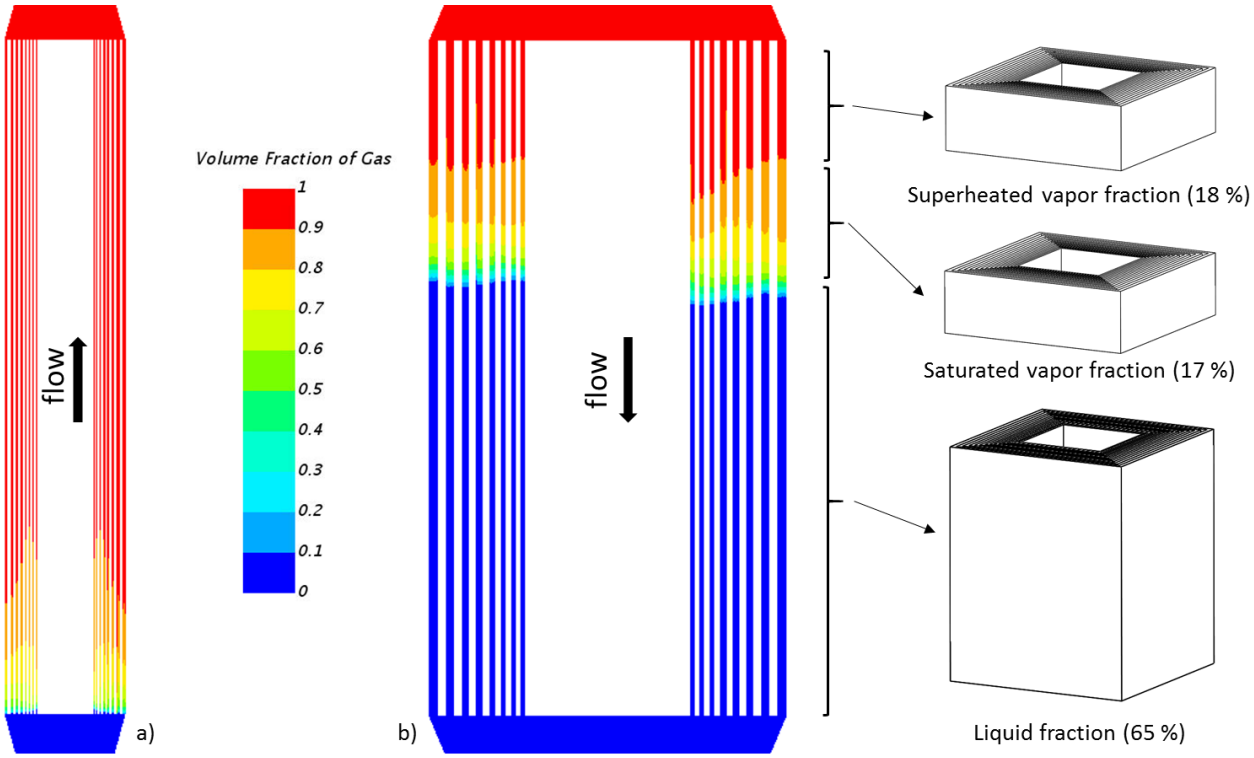

Figure 7: Vapor volume fraction in the evaporator (left) and inside the condenser (right)

NOMENCLATURE

Variables

α	convective heat transfer coefficient	(W/m^2 K)
h	enthalpy	(kJ/kg)
p	pressure	(bar)
s	entropy	(kJ/kg K)
T	temperature	(K)
z	coordinate	(-)

Acronyms

FF	Fluid Film
ORC	Organic Rankine Cycle
P&ID	Piping and Instrumentation Diagram
VOF	Volume of Fluids
WOM	Whole ORC Model

Subscripts

IN	inlet section	PC	Phase Change
OUT	outlet section	wall	wall (referred to the location)

REFERENCES

Macchi E., Astolfi M. (2016). *Organic Rankine Cycle (ORC) Power Systems, Technologies and Applications*. Duxford: Woodhead Publishing Series in Energy: Number 107; 2016.

Bhutta M.M., Hayat N., Bashir M.H., Khan A.R., Ahmad K.N., Khan S. (2012). CFD applications in various heat exchangers design: A review. *Appl. Therm. Eng. 32*,1-12.

Chang J.C., Chang C.W., Hung T.C., Lin J.R., Huang K.C. (2014). Experimental study and CFD approach for scroll type expander used in low-temperature organic Rankine cycle. *Appl. Therm. Eng. 73*,1444-452.

Morini M., Pavan C., Pinelli M., Romito E., Suman A. (2015). Analysis of a scroll machine for micro ORC applications by means of a RE/CFD methodology. *Appl. Therm. Eng. 80*, 132-40.

Song P., Wei M., Shi L., Danish S.N., Ma C. (2015) A review of scroll expanders for organic Rankine cycle systems. *Appl Therm Eng. 75*, 54-64.

Ziviani D., Gusev S., Lecompte S., Groll E.A., Braun J.E., Horton W.T., van den Broek M., De Paepe M. (2016). Characterizing the performance of a single-screw expander in a small-scale organic Rankine cycle for waste heat recovery. *Appl Energy 181*, 155-70.

Casari N., Suman A., Morini M., Pinelli M. (2017a). Real Gas Expansion with Dynamic Mesh in Common Positive Displacement Machines. *Energy Procedia, 129*, 248-55.

Casari N., Suman A., Ziviani D., van den Broek M., De Paepe M., Pinelli M. (2017b). Computational Models for the Analysis of positive displacement machines: Real Gas and Dynamic Mesh. *Energy Procedia, 129*, 411-18.

Suman A., Randi S., Casari N., Pinelli M., Nespoli L. (2017). Experimental and Numerical Characterization of an Oil-Free Scroll Expander. *Energy Procedia, 129,* 403-10.

Papes I., Degroote J., Vierendeels J. (2015) New insights in twin screw expander performance for small scale ORC systems from 3D CFD analysis. *Appl. Therm. Eng. 91*, 535-46.

Ziviani D., Suman A., Gabrielloni J., Pinelli M., De Paepe M. (2016) CFD Approaches To A Single-Screw Expander. *Proceeding of the 23rd International Compressor Engineering Conference at Purdue, 1488.*

Del Campo D., Castilla R., Raush G.A., Gamez-Montero P.J., Codina E. (2012). Numerical Analysis of External Gear Pumps Including Cavitation. *J. Fluids Eng. 134*(8).

Castilla R., Gamez-Montero P. J., Ertürk N., Vernet A., Coussirat M., Codina E. (2010). Numerical simulation of turbulent flow in the suction chamber of a gear pump using deforming mesh and mesh replacement. *Int. J. Mech. Sci. 52*, 1334-342.

Donghong W., Xuesheng L., Zhen L., Jianming G. (2008). Dynamic modeling and simulation of an Organic Rankine Cycle (ORC) system for waste heat recovery. *Appl. Therm. Eng. 28*, 1216-224.

Dickes R., Dumont O., Daccord R., Quoilin S., Lemort V. (2017). Modelling of organic Rankine cycle power systems in off-design conditions: an experimentally-validated comparative study. *Energy, 123*, 710-27.

Liuchen L., Yu P., Tong Z., Naiping G. (2017). Numerical predicting the dynamic behavior of heat exchangers for a small-scale Organic Rankine Cycle. *Energy Procedia, 129*, 419-26.

Desideri A., van den Broek M., Gusev S., Lemort V., Quoilin S. (2014) Experimental Campaign and Modelling of a Low-capacity Waste Heat Recovery System Based on a Single Screw Expander. *Proceeding of the 22nd International Compressor Engineering Conference at Purdue, 1451.*

Casari N., Suman A., Ziviani D., Morini M., Pinelli M. (2017c) Virtual model for ORC – Whole ORC Modeling: WOM. *Proceedings of ECOS 2017 30th International Conference on Efficiency, Cost, Optimisation, Simulation and Environmental Impact of Energy Systems*, San Diego, CA

Ancona M.A., Bianchi M., Branchini L., De Pascale A., Melino F., Orlandini V., Ottaviano S., Peretto A., Pinelli M., Spina P.R., Suman A. (2016). A Micro-ORC Energy System: Preliminary Performance and Test Bench Development, *Energy Procedia, 101*, 814-21.

Bianchi M., Branchini L., De Pascale A., Orlandini V., Ottaviano S., Peretto A., Melino F., Pinelli M., Spina P.R., Suman A. (2017). Experimental Investigation with Steady-State Detection in a Micro-ORC Test Bench. *Energy Procedia, 126,* 469-76.

Bianchi M., Branchini L., De Pascale A., Orlandini V., Ottaviano S., Pinelli M., Spina P.R., Suman A. (2017). Experimental Performance of a Micro-ORC Energy System for Low Grade Heat Recovery. *Energy Procedia, 129,* 899-906

Hirt, C.W., Nichols, B.D. (1981). Volume of fluid (VOF) method for the dynamics of free boundaries. *J Comput Phys*, 39(1), 201-25.

Spalart P., Allmaras S.A. (1992). One-Equation Turbulence Model for Aerodynamic Flows. AIAA. DOI: 10.2514/6.1992-439.

ACKNOWLEDGMENTS

The research was partially supported by the Italian Ministry of Economic Development within the framework of the Program Agreement MSE-CNR “Micro co/tri generazione di Bioenergia Efficiente e Stabile (Mi-Best)”.